ACS POLYMERS Au
AN OPEN ACCESS JOURNAL OF THE AMERICAN CHEMICAL SOCIETY

pubs.acs.org/polymerau

Article

All-Peptide-Based Polyion Complex Vesicles: Facile Preparation and Encapsulation of the Protein in Active Form

Seiya Fujita, Kousuke Tsuchiya,* and Keiji Numata*

Cite This: *ACS Polym. Au* 2021, 1, 30–38

Read Online

ACCESS | Metrics & More | Article Recommendations | Supporting Information

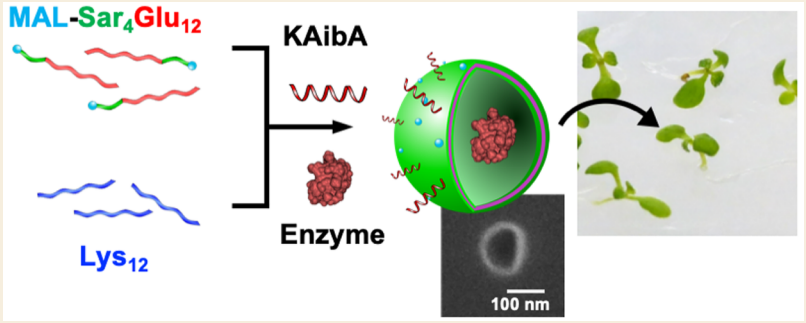

ABSTRACT: The polyion complex vesicle (PICsome) is a promising platform for bioactive molecule delivery as well as nanoreactor systems. In addition to anionic and cationic charged blocks, a hydrophilic poly(ethylene glycol) (PEG) block is mostly employed for PICsome formation; however, the long-term safety of the PEG component in vivo is yet to be clarified. In this study, we developed novel PEG-free PICsome comprising all peptide components. Instead of the PEG block, we selected the sarcosine (Sar) oligomer as a hydrophilic block and fused it with anionic oligo(L-glutamic acid). Mixing the Sar-containing anionic peptide with cationic oligo(L-lysine) resulted in the formation of stable vesicles. The peptide-based PICsome was able to encapsulate a model protein in its hollow structure. After modification of the surface with a cell-penetrating peptide, the protein-encapsulated PICsome was successfully delivered into plant cells, indicating its promised for application as a biocompatible carrier for protein delivery.

KEYWORDS: *Polyion complex vesicle, PICsome, Peptide, Protein delivery, Plant*

INTRODUCTION

Polymeric vesicles which possess a hollow structure filled with aqueous media are promising materials for efficient molecular delivery in medical applications.[1−4] Similar to liposomes in living cells, cargo molecules are enclosed in their hollow structure without sacrificing their intact functions. To date, many types of amphiphilic block copolymers have been developed for nanocarriers and/or nanoreactors to deliver various exogenic biomolecules into living tissues/cells.[5,6] In particular, polyion complex vesicles, named PICsome, have emerged as practical polymeric carriers to deliver pharmaceutical molecules and also nanoreactors for confined selective reactions in vivo.[7,8] General structures for polymeric components of PICsome are composed of hydrophilic polymers, representatively, poly(ethylene glycol) (PEG), and ionic polymers with complementary charges. Enzymes encapsulated in PICsome were durable against proteolysis and hence preserved their functionality for a long period in a living body.[9,10]

Peptides are capable of serving as functional components for material delivery platforms since a wide variation in their primary structures allows us to design a great number of functional sequences. In addition, peptides are biodegradable and biocompatible, assuring noncytotoxic applications. We have focused on material delivery into plants using peptide-based carriers because the direct delivery of proteins into plant cells can confer exotic functions or traits on plants without unfavorable permanent genetic modifications, which limit the practical use of plants for foods and material production. Recently, we reported that PICsome were prepared by mixing cationic and anionic oligopeptides fused with tetra(ethylene glycol) (TEG) and that the resulting vesicles can serve as a carrier to deliver a functional enzyme, neomycin phosphotransferase II (NPTII), into plants after the modification with an appropriate cell-penetrating peptide (CPP) with a sophisticated design to penetrate the plant cell wall/membrane.[11] The encapsulation in the peptide-based PICsome enabled NPTII to remain stable and functional for a long

Received: April 16, 2021
Published: June 21, 2021

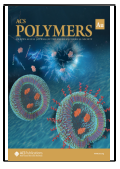

period in plant cells, imparting a resistance against antibiotics such as kanamycin to plants. Thus, the combination of short peptides with an ability to form a complex by electrostatic interaction is beneficial for the components of a PICsome.

PEG is one of the most widely used polymeric components in material delivery platforms because it shows the physiologically inert nature which reduces immunogenicity and nonspecific interaction with biomolecules.[12,13] PICsome and other polymeric vesicles generally contain PEG as a hydrophilic component to accomplish long circulation time in their material delivery use in vivo. However, due to the long-term stability of the PEG backbone, whether the duration of PEG component is safe in living organism is still controversial.[14,15] Recently, other biologically inert polymers with a resistance to nonspecific biomolecule absorption have been employed as an alternative to the PEG component.[16] Polypeptides consisting of sarcosine (Sar) residues are known as hydrophilic biocompatible polymers and have been applied to the polymer micelles,[17−20] dendrimers,[21,22] and polymersomes[23−27] as a biocompatible carrier for drug delivery. A nonproteinogenic amino acid Sar is naturally abundant in living organisms.[28,29] Therefore, the Sar-rich polypeptides are degradable after a certain period of proteolytic resistance and thereby show low negative effect in vivo.[30,31]

Here, we newly designed cationic and anionic peptides for preparation of all-peptide-based PICsome (Figure 1). We

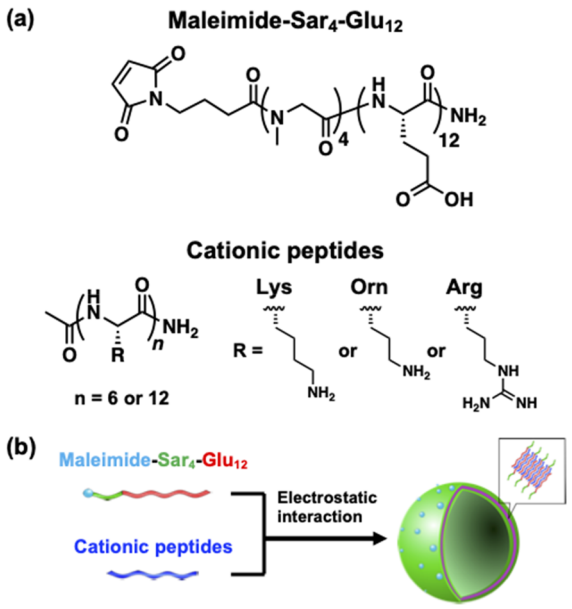

Figure 1. Schematic illustration of PICsome formation with reactive maleimide groups on the surface by mixing anionic and cationic peptides.

demonstrated that PICsome was successfully formed by mixing the Sar-containing anionic peptide with a cationic peptide and utilized for the encapsulation of proteins in its hollow structure. After the conjugation with CPP, the resulting PICsome was found to encapsulate and deliver a model enzyme into plant cells. The peptide-based PICsome is a promising PEG-free platform for material delivery and/or as a nanoreactor in living systems.

EXPERIMENTAL SECTION

Materials

A maleimide (MAL)-terminated anionic peptide, MAL-Sar_4Glu_{12} (MAL-XXXXEEEEEEEEEEEE-NH_2, X = Sar), cationic peptides, Lys_{12} (Ac-KKKKKKKKKKKK-NH_2), Orn12 (Ac-UUUUUUUUUUUU-NH2, U = ornithine), and Arg_{12} (Ac-RRRRRRRRRRRR-NH_2), and a cell-penetrating peptide, KAibA (Ac-CKXAKXAKXA-NH_2, X = 2-aminoisobutyric acid, Aib), were synthesized using Fmoc-based solid-phase peptide synthesis by the Research Resources Division of RIKEN Center for Brain Science (Wako, Japan). The N- and C-termini of all peptides were terminated with acetyl and amide groups, respectively, except for the MAL group at the N-terminal of MAL-Sar_4Glu_{12}. The purity of each peptide was determined as greater than 90% by RP-HPLC analysis (Figure S1). A cationic peptide Lys_6 (H-KKKKKK-OEt) was prepared by chemo-enzymatic polymerization of N_ε-Boc-protected Lys ethyl ester followed by deprotection, according to the previous report.[11] Ribonuclease A (RNase) was purchased from Nacalai Tesque Inc. (Kyoto, Japan) and labeled with rhodamine B (RhB) by reacting RNase (10 mg mL^{-1}) in 100 mM carbonate buffer (pH 9.0) with rhodamine B isothiocyanate (10 mg mL^{-1}) in *N*,*N*-dimethylformamide at 25 °C for 1 h. The resulting solution was centrifuged (5000*g*, 1 min), and the RhB-labeled RNase was purified by passing the supernatant through a PD-10 column (Cytiva, Marlborough, MA). The final concentration of RhB-labeled RNase was determined using a Microplate BCA protein assay kit (Thermo Fisher Scientific, Waltham, MA) for further experiments. Wild-type (Col-0) or transgenic (YFP-expressing) *Arabidopsis thaliana* (a model dicot plant species) seedling was used for PICsome delivery experiments. The seeds of *A. thaliana* were germinated on plates with 0.8% agarose gel containing a half Murashige and Skoog (MS) medium and grown in an incubator (Biotron, NK systems, Osaka, Japan) under daylength conditions of 16 h of light/8 h of dark at 22 °C. The seedlings 4 days after germination were used for the experiments.

Preparation of PICsome

A solution of MAL-Sar_4Glu_{12} in 1 mM Bis-Tris buffer (pH 7.0) was added into 500 mM sodium acetate buffer (pH 5.0), and the resulting solution was lyophilized. The dried solid was added in ethanol, and the dispersion was centrifuged (9000*g*, 10 min) three times to collect the sodium salt of MAL-Sar_4Glu_{12} as a precipitated pellet. A solution of the sodium salt of MAL-Sar_4Glu_{12} (1 mg) in 2 mM Bis-Tris buffer (248 μL, pH 7.0) was mixed with a solution of Lys_{12}, Lys_6, Orn_{12}, or Arg_{12} (1 mg) in Milli-Q (313, 624, 350 μL, respectively) at a negative/positive charge (N/P) ratio = 1/1.

Dynamic Light Scattering (DLS) Measurement

The hydrodynamic diameter of the assemblies prepared by mixing anionic and cationic peptides was characterized by DLS measurement using a Zetasizer Nano ZS instrument (Malvern Instruments Ltd., Worcestershire, UK). After the solutions of anionic and cationic peptides were mixed at a N/P ratio = 1/1, the mixture was incubated at 25 °C for 1 h. The DLS measurement was performed on the solution (100 μL) in a plastic cell (DTS1070) using a 633 nm He−Ne laser at 25 °C with a backscatter detection angle of 173° to estimate hydrodynamic diameter as a *Z*-average size and polydispersity index (PDI). The measurement was replicated three times, and the data were averaged to determine the standard deviation.

Evaluation of Salt Stability of PICsome

A solution of MAL-Sar_4Glu_{12} in Bis-Tris buffer (50 μL, 500 μM, pH 7.0) was then mixed with 50 μL of a solution of Lys_{12} in Milli-Q and incubated at 25 °C for 10 min. Then, a solution of NaCl with a various concentration (1−100 mM) was added to the mixture solution. After 30 min incubation, the DLS measurement was performed on the solution (100 μL) in a plastic cell (DTS1070) using a 633 nm He−Ne laser at 25 °C with a backscatter detection angle of 173° to estimate hydrodynamic diameter as a *Z*-average size and PDI. The measurement was replicated three times, and the data were averaged to determine the standard deviation.

https://doi.org/10.1021/acspolymersau.1c00008
ACS Polym. Au 2021, 1, 30−38

Evaluation of pH Stability of PICsome

A solution of MAL-Sar_4Glu_{12} in Bis-Tris buffer (50 μL, 500 μM, pH 7.0) was then mixed with 50 μL of a solution of Lys_{12} in Milli-Q and incubated at 25 °C for 10 min. Then, an aqueous solution of HCl or NaOH was added to the mixture solution until the solution reached to desired pH range of 5 to 9. After 30 min incubation, the DLS measurement was performed on the solution (100 μL) in a plastic cell (DTS1070) using a 633 nm He−Ne laser at 25 °C with a backscatter detection angle of 173° to estimate hydrodynamic diameter as a *Z*-average size and PDI. The measurement was replicated three times, and the data were averaged to determine the standard deviation.

Field-Emission Scanning Electron Microscopy (FE-SEM)

Morphology of the assemblies prepared by mixing the anionic and cationic peptides was observed by FE-SEM. A solution of the peptide mixture (0.5 μL) was deposited on a silicon wafer and lyophilized. The sample was subjected to FE-SEM observation using GeminiSEM 300 (Carl Zeiss, Oberkochen, Germany) with an acceleration voltage of 1 kV. For the cross-sectional SEM, the sample solution was mixed with a low-melting agarose at 1/1 in volume. The mixture was solidified at 25 °C for 30 min and dehydrated by immersing in methanol and propylene oxide. The agarose gel was embedded in an epoxy resin (EPON 812, TAAB Laboratories Equipment Ltd., Berkshire, UK) and incubated at 60 °C for 2 days. The resin was cut with a microtome (POWERTOME, RMC product, India) into a slice with a thickness of 100 nm. The section was stained with osmium chloride for 5 min and lead acetate for 30 min. After being dried at 25 °C, the sample was coated with carbon prior to FE-SEM observation with an acceleration voltage of 4 kV.

Encapsulation of RNase in PICsome

A solution of RhB-labeled RNase in 10 mM Bis-Tris buffer (1.0 μL, 1.0 mg mL^{-1}, pH 7.0) was mixed with 50 μL of a solution of MAL-Sar_4Glu_{12} in Bis-Tris buffer (500 μM, pH 7.0). The mixture was then mixed with 50 μL of a solution of Lys_{12} in Milli-Q and incubated at 25 °C for 10 min. The solution was dialyzed against 1 mM Bis-Tris buffer (pH 7.0) using a cellulose membrane (MWCO: 100 kDa) for 4 h to remove free RhB-labeled RNase. To determine the incorporation ratio of RhB-labeled RNase in PICsome from the solution, the final solution was subjected to sodium dodecyl sulfate polyacrylamide gel electrophoresis (SDS-PAGE). After lyophilization of the final solution, Laemmli SDS-PAGE sample buffer (10 μL) was added to the solid sample and heated at 95 °C for 5 min. After 10 μL of the denatured solution was loaded in 8−16% Mini-PROTEANTGX gels (Bio-Rad, Hercules, CA), electrophoresis was run at 100 V for 50 min. The resulting gel was covered with isopropyl alcohol fixing solution with a gentle shaking and then stained with using a SilverXpress (Invitrogen, Carlsbad, CA). The concentration of RhB-labeled RNase was estimated by analyzing the stained band by ImageJ using a standard calibration curve.

Encapsulation of RNase in the Assembly Formed from Orn_{12}/MAL-Sar_4Glu_{12}

A solution of MAL-Sar_4Glu_{12} in Bis-Tris buffer (50 μL, 500 μM, pH 7.0) was then mixed with 50 μL of a solution of Orn_{12} in Milli-Q and incubated at 25 °C for 10 min. Then, a solution of RhB-labeled RNase in 10 mM Bis-Tris buffer (1.0 μL, 1.0 mg mL^{-1}, pH 7.0) was added to the mixture solution and incubated for 30 min. The solution was dialyzed against 1 mM Bis-Tris buffer (pH 7.0) using a cellulose membrane (MWCO: 100 kDa) for 4 h to remove free RhB-labeled RNase. The incorporation ratio of RhB-labeled RNase in assemblies from the solution was determined according to the procedure described above.

Encapsulation of RNase in Preassembled PICsome

A solution of MAL-Sar_4Glu_{12} in Bis-Tris buffer (50 μL, 500 μM, pH 7.0) was mixed with 50 μL of a solution of Lys_{12} in Milli-Q and incubated at 25 °C for 10 min. Then, a solution of RhB-labeled RNase in 10 mM Bis-Tris buffer (1.0 μL, 1.0 mg mL^{-1}, pH 7.0) was added to the mixture solution and incubated for 30 min. The solution was dialyzed against 1 mM Bis-Tris buffer (pH 7.0) using a cellulose membrane (MWCO: 100 kDa) for 4 h to remove free RhB-labeled RNase. The incorporation ratio of RhB-labeled RNase in preassembled PICsome from the solution was determined according to the procedure described above.

Fluorescent Correlation Spectroscopy (FCS)

The FCS measurement was performed on the solution of RhB-labeled RNase or citrine in the absence and presence of PICsome using a confocal laser scanning microscope LSM880 (Carl Zeiss, Oberkochen, Germany) with a laser of 488 nm. The fluctuation of the fluorescent intensity from RhB or citrine was measured to obtain the autocorrelation function $G(t)$. The experimental autocorrelation curve was fitted using a following function:

$$G(t) = 1 + \frac{1}{N} \times \frac{1}{\left(1 + \frac{t}{\tau}\right)\sqrt{1 + \frac{1}{k^2}\cdot\frac{t}{\tau}}} \times \left(\frac{1 + Fe^{t/\tau_{trip}}}{1 - F}\right)$$

where N is number of molecules, t is correlation time, τ is the diffusion time of component, k is structural constant, F is the fraction of particles that have entered the triplet state, and τ_{trip} is the relaxation time of the corresponding triplet state. The fitting was performed by ZEN 2.3 SP1 operating software (Carl Zeiss, Oberkochen, Germany). The diffusion coefficient and hydrodynamic diameter of RhB-labeled RNase in the absence and presence of PICsome were estimated from the fitting curves.

Evaluation for Enzyme Activity of RNase

Enzyme activity of RNase encapsulated in PICsome was determined by RNaseAlert lab test kit v2 (Invitrogen, Carlsbad, CA). A substrate solution was diluted 10-fold with 1 mM Bis-Tris buffer, and 2.5 μL of this solution was mixed with 22.5 μL of RNase or RNase-encapsulated PICsome solution (17.7 μg mL^{-1}). The mixture was reacted at 25 °C for 5 min. After the reaction, the fluorescence from the reaction product at 520 nm was measured by a FP-8500 spectrofluorometer (JASCO, Tokyo, Japan).

Modification of PICsome with CPP (KAibA)

A solution of RhB-labeled RNase in 10 mM Bis-Tris buffer (1 μL, 1 mg mL^{-1}, pH 7.0) was mixed with a solution of MAL-Sar_4Glu_{12} in Bis-Tris buffer (50 μL, 500 μM, pH 7.0). Then, the solution was mixed with a solution of Lys_{12} in Milli-Q (50 μL) and incubated at 25 °C for 10 min. After the solution was dialyzed against 1 mM Bis-Tris buffer (pH 7.0) for 2 h, KAibA (0.25 equiv to the MAL group) was added and the mixture was stirred at 25 °C for 30 min. The reaction mixture was further dialyzed against 1 mM Bis-Tris buffer (pH 7.0) for 2 h prior to the infiltration into plant seedlings. The conversion of the MAL group was calculated from reverse-phase high-performance liquid chromatography (RP-HPLC) analyses using a HPLC system consisting of autosampler AS-2055, gradient pump PU2089, column oven CO-4060, UV/vis detector UV-4075, and quaternary gradient pump PU-2089 Plus (JASCO, Tokyo, Japan) using the YMC-Triart C18 column (particle size 5 μm, 150 × 3 mm, YMC, Kyoto, Japan) with a flow rate of 1 mL min^{-1} at 25 °C. Boc-Gly was used for an internal standard. The click reaction mixture with Boc-Gly was injected and eluted by a mixed mobile phase with a linear gradient of CH_3CN/water containing 0.1% TFA (5/95 to 52.5/47.5 over 47.5 min). The conversion of MAL groups was calculated by comparing the peak area before and after the reaction.

Infiltration of RNase-Encapsulated PICsome into Plants

Prior to infiltration into *A. thaliana* seedlings, RhB-labeled RNase encapsulated in PICsome (RNase@PICsome) or CPP-modified PICsome (RNase@CPP-PICsome) was prepared according to the procedure described above. Then, 4-day-old seedlings of *A. thaliana* were added to a solution of RNase, RNase@PICsome, or RNase@CPP-PICsome in a 2 mL microtube. The microtube was subjected to vacuum at −0.08 MPa for 1 min and pressurized at 0.08 MPa for 1 min. The seedlings were then transferred on agarose gel containing half MS media and grown for 1 day. The seedlings were stained with calcofluor white (0.1 g L^{-1}) for 10 min and subjected to confocal laser scanning microscopy (CLSM) observation by LSM880 (Carl Zeiss,

https://doi.org/10.1021/acspolymersau.1c00008
ACS Polym. Au 2021, 1, 30−38

Oberkochen, Germany). Images were acquired at an excitation wavelength of 405 nm (for calcofluor white) and 561 nm (for RhB) and visualized under a 63× oil-immersion objective. Colocalization analysis of micrographs was performed using the Zen 2.3 SP1 operating software (Carl Zeiss).

Preparation of Citrine-Encapsulated CPP-PICsome

A solution of citrine in 10 mM Bis-Tris buffer (1 μL, 1 mg mL^{-1}, pH 7.0) was mixed with a solution of MAL-Sar$_4$Glu$_{12}$ in Bis-Tris buffer (50 μL, 500 μM, pH 7.0). Then, the solution was mixed with a solution of Lys$_{12}$ in Milli-Q (50 μL) and incubated at 25 °C for 10 min. After the solution was dialyzed against 1 mM Bis-Tris buffer (pH 7.0) for 3 h, KAibA (0.25 equiv. to the MAL group) was added and the mixture was reacted at 25 °C for 30 min. The reaction mixture was further dialyzed against 1 mM Bis-Tris buffer (pH 7.0) for 3 h prior to the infiltration into plant seedlings.

Infiltration of Citrine-Encapsulated PICsome into Plants

Prior to infiltration into *A. thaliana* seedlings, citrine encapsulated in CPP-modified PICsome (citrine@CPP-PICsome) was prepared according to the procedure described above. Ten 4-day-old seedlings of *A. thaliana* were added to a solution of citirine@CPP-PICsome in a 2 mL microtube. The microtube was subjected to vacuum at −0.08 MPa for 1 min and pressurized at 0.08 MPa for 1 min. The seedlings were then transferred on agarose gel containing half MS media and grown for 1 day. The seedlings were stained with calcofluor white (0.1 g L^{-1}) for 10 min and subjected to CLSM observation by LSM880 (Carl Zeiss, Oberkochen, Germany). Images were acquired at excitation wavelength of 405 nm (for calcofluor white) and 514 nm (for Citrine) and visualized under a 63× oil-immersion objective. Colocalization analysis of micrographs was performed using the Zen 2.3 SP1 operating software (Carl Zeiss).

RESULTS AND DISCUSSION

First, we clarified the best combination of amino acid residues in cationic and anionic peptides for PICsome formation and optimized the preparation condition. We selected three types of oligopeptides with a homosequence of L-amino acids, Lys$_{12}$, Orn$_{12}$, and Arg$_{12}$, as cationic peptides. On the other hand, a fused peptide consisting of maleimide-terminated oligosarcosine and oligo(L-glutamic acid), MAL-Sar$_4$Glu$_{12}$, was synthesized as an anionic peptide. These short peptides were conveniently synthesized by solid-phase peptide synthesis. We already reported that the 6 amino acid residues are sufficient for the formation of PICsome.[11] Judging from the peptide length for the easy synthesis as well as the stability of the resultant vesicles, we decided the number of charged amino acid residues as 12 for both peptides. The oligosarcosine block in the anionic peptide forms hydrophilic layers of PICsome instead of conventional PEG block. According to previous report, the volume fraction of oligosarcosine in the peptide should be less than 10% for vesicle formation, otherwise forming a micellar morphology.[32] Taking this into account, the number of Sar residues was fixed at 4 to Glu residues of 12. Furthermore, the maleimide group was introduced at the N-terminal to modify the surface of PICsome with functional peptides such as a CPP. A solution of MAL-Sar$_4$Glu$_{12}$ was mixed with various cationic peptides at a N/P ratio of 1/1 and incubated for 30 min, and the *Z*-average diameter and size distribution of the particles was estimated by DLS, as shown in Table 1 and Figure S2. When Lys$_{12}$ or Orn$_{12}$ was mixed with MAL-Sar$_4$Glu$_{12}$ at an equimolar ratio between cationic and anionic charges, the spherical assembly was obtained with a hydrodynamic diameter ranging from 111 to 330 nm at 100−500 μM concentration of peptides. The hydrodynamic diameter of PICsome is dependent on the peptide concentration. This can be explained by the number of peptides in a unit space proportionally increasing with an increase in the peptide concentration, resulting in an increase in the surface area and size of assemblies.[7] There was no significant change in hydrodynamic diameter for 8 h (Figure S3). Salt and pH stability of PICsome were evaluated by DLS measurement (Tables S1 and S2). PICsome maintained the size at low salt concentration or at neutral and basic condition, whereas PICsome was aggregated in the presence of a high concentration of NaCl or at lower pH. For higher stability of PICsome, the cross-link of the PICsome membrane is necessary; however, the cross-linking of PICsome in this study failed under the reported condition in the previous work. In the future, we will find the appropriate cross-linking condition for PICsome to achieve higher stability in practical use of material delivery. Observation by FE-SEM revealed that a spherical assembly was obtained for both of the combination, Lys$_{12}$/MAL-Sar$_4$Glu$_{12}$ and Orn$_{12}$/MAL-Sar$_4$Glu$_{12}$ (Figure 2a,b). For the combination of Lys$_{12}$/MAL-Sar$_4$Glu$_{12}$, the spherical assembly was formed at concentrations ranging from 100 to 1000 μM. The hydrodynamic diameter of the assembly was 111−205 nm and the PDI value was prone to increase as the peptide solution was diluted. At the best concentration of 500 μM, the spherical nanoassembly of 122 nm with a narrow size distribution was obtained. In the case of Orn$_{12}$/MAL-Sar$_4$Glu$_{12}$, the assembly formed at lower concentration (100 μM) showed smaller hydrodynamic diameter (167 nm) and PDI (0.109). In contrast, the combination between Arg$_{12}$ and MAL-Sar$_4$Glu$_{12}$ provided a large assembly with a diameter of 8.6 μm by DLS. The morphology of the assembly obtained from Arg$_{12}$/MAL-Sar$_4$Glu$_{12}$ was large aggregates with a sheet-like structure (Figure S4). The bulky guanidinium moiety in the side chain of Arg residue is assumed to disturb the formation of an ordered lamellar structure composed of cationic and anionic peptides. In addition, electrostatic interaction between Glu and Arg residues is so strong that results in the formation of large aggregates, according to a previous report.[33]

Table 1. Physicochemical Properties of Polyion Complex Assembly Prepared by Mixing MAL-Sar$_4$Glu$_{12}$ and Various Cationic Peptides

cationic peptide	[peptide] (μM)	diameter[a] (nm)	PDI[b]
Lys$_{12}$	1000	205 ± 6	0.196
Lys$_{12}$	500	122 ± 1	0.219
Lys$_{12}$	300	111 ± 2	0.311
Lys$_{12}$	100	122 ± 15	0.484
Lys$_6$[c]	500	186 ± 2	0.299
Orn$_{12}$	500	330 ± 26	0.298
Orn$_{12}$	100	167 ± 1	0.109
Arg$_{12}$	500	8631 ± 1574	0.826

[a]Hydrodynamic diameter determined by DLS (n = 3). [b]Polydispersity index determined by DLS. [c]Two equivalents to MAL-Sar$_4$Glu$_{12}$.

To confirm that the obtained polyion complex assembly possesses a hollow structure, we carried out the FE-SEM observation on their cross section. The spherical assemblies obtained from Lys$_{12}$/MAL-Sar$_4$Glu$_{12}$ and Orn$_{12}$/MAL-Sar$_4$Glu$_{12}$ were embedded in an epoxy resin, and a thin slice of the resin was prepared by microtome for FE-SEM observation. The cross-sectional images of spherical assemblies are shown in Figure 2. The assembly from Lys$_{12}$/MAL-Sar$_4$Glu$_{12}$ distinctly exhibited a hollow structure in the

https://doi.org/10.1021/acspolymersau.1c00008
ACS Polym. Au 2021, 1, 30−38

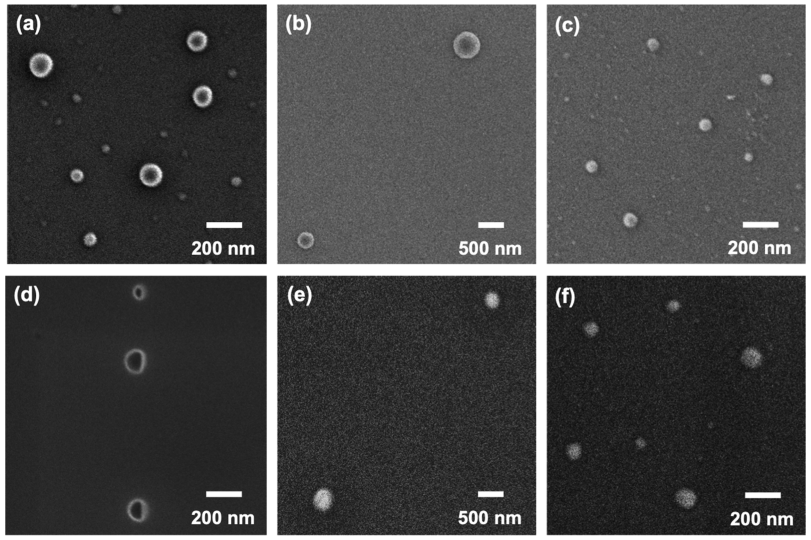

Figure 2. (a–c) FE-SEM images of polyion complex assemblies formed by mixing cationic and anionic peptides: (a) Lys_{12}/ MAL-Sar_4Glu_{12}, (b) Orn_{12}/ MAL-Sar_4Glu_{12}, and (c) Lys_6/ MAL-Sar_4Glu_{12}. (d–f) Cross-sectional FE-SEM images of spherical assemblies obtained from (d) Lys_{12}/ MAL-Sar_4Glu_{12}, (e) Orn_{12}/ MAL-Sar_4Glu_{12}, and (f) Lys_6/ MAL-Sar_4Glu_{12}.

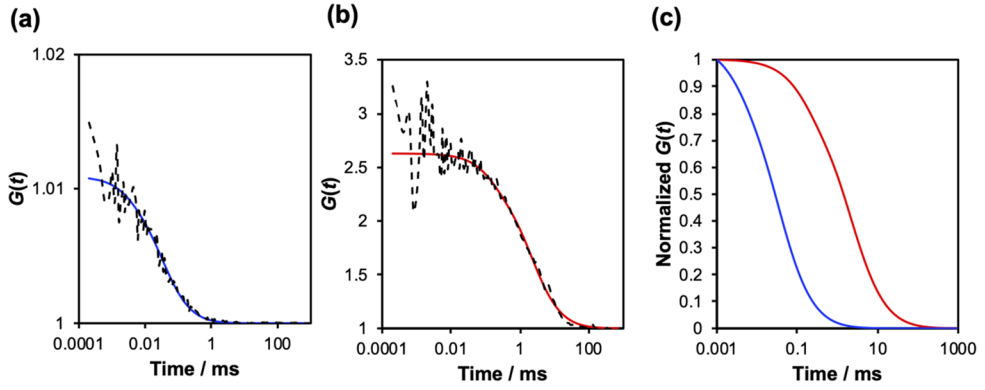

Figure 3. (a,b) Experimental autocorrelation functions (broken line) and fitting curves (solid line) obtained by FCS for RhB-labeled RNase in the (a) absence and (b) presence of PICsome and (c) normalized autocorrelation fitting curves for RhB-labeled RNase in the absence (blue) and presence (red) of PICsome.

spherical assembly, confirming the formation of PICsome (Figure 2d). The thickness of the membrane was approximately 17 nm in FE-SEM images, which is comparable to the length of two peptide molecules with a fully extended structure. Therefore, we assumed that this assembly consists of a bilayer membrane.

In contrast, the assembly from Orn_{12}/MAL-Sar_4Glu_{12} also had a spherical shape, but the hollow structure was not observed in the cross-sectional FE-SEM image (Figure 2e). These results indicate that cationic peptides with longer aliphatic side chains favor the formation of vesicles because the higher hydrophobicity caused by longer methylene chains results in a more stable assembly of a polyion complex in lamellar structures, as reported in the previous study.[32] In addition, when Lys_{12} was substituted with 2 equiv of Lys_6, the assembly from Lys_6/MAL-Sar_4Glu_{12} showed a spherical shape without a hollow inside, even with a same amino acid composition as Lys_{12}/MAL-Sar_4Glu_{12} (Figure 2f). The combination of Orn_{12}/MAL-Sar_4Glu_{12} or Lys_6/MAL-Sar_4Glu_{12} favors polyion complex micelle formation rather than PICsome. This finding indicates that the strictly same main chain length in cationic and anionic peptides as well as an optimum side chain length should be required for the formation of vesicles.

We investigated the availability of the obtained PICsome for a material delivery platform. The peptide-based PICsome was prepared in the presence of a RhB-labeled model protein, ribonuclease A (RNase), as a guest molecule. After the removal of free RNase by dialysis, the colloidal behavior of PICsome was analyzed by FCS. FCS measures the diffusion time of a fluorescent molecule. The apparent diffusion time of a fluorescent molecule increases when the fluorescent molecule is encapsulated in the hollow interior of the PICsome. For FCS measurements, RNase was labeled with RhB isothiocyanate according to a previous report. The autocorrelation function $G(t)$ was obtained for RNase in an aqueous solution in the absence and presence of PICsome (Figure 3). By fitting the $G(t)$ curve, the free RNase is dispersed in a unimodal fluctuation mode with a diffusion coefficient of 85.4 $\mu m^2/s$. On the other hand, RNase in the presence of PICsome also showed the $G(t)$ curve with a unimodal fluctuation mode but with a smaller diffusion coefficient of 2.22 $\mu m^2/s$ (Figure 3c), indicating that no free RNase remained after the dialysis. In addition, the hydrodynamic diameter calculated from the diffusion coefficient for RNase with PICsome was 220 nm,

https://doi.org/10.1021/acspolymersau.1c00008
ACS Polym. Au 2021, 1, 30–38

which corresponds to that of PICsome obtained from DLS measurement. After encapsulation of RNase into PICsome, the average number of RhB-modified RNase decreased from 3.7 to 0.63 in a unit volume of the FCS measurement at the same concentration of RNase. It means that approximately 6 RhB-modified RNase molecules were entrapped in one vesicle component.

Encapsulation efficiency of RNase into PICsome was estimated by electrophoresis (Figure 4). When the free

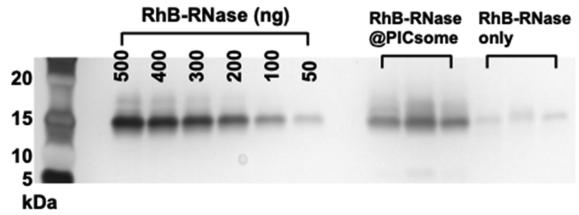

Figure 4. Quantification of RhB-labeled RNase incorporated in PICsome using Lys_{12}/MAL-Sar_4Glu_{12} by silver staining. The sodium dodecyl sulfate polyacrylamide gel electrophoresis (SDS-PAGE) loaded with the solution of RhB-labeled RNase (1 μg) dialyzed against 1 mM Bis-Tris buffer in the presence and absence of PICsome.

RNase was dialyzed using a cellulose membrane with molecular weight cutoff of 100 kDa, RNase could be completely removed from the solution after 4 h (Figure S5). In contrast, in the presence of PICsome, 17.7% of RNase in the solution remained after dialysis for 4 h (Figure S6). In addition, when RNase was mixed with preassembled PICsome, 97.8% of RNase was removed by dialysis (Figure S8). These results indicate that RNase is not presented on the surface of PICsome by nonspecific adsorption or undesired reaction of maleimide with thiol, and that RNase was incorporated into PICsome by mixing the anionic and cationic peptides in the presence of RNase. We evaluated the encapsulation of RNase using MAL-Sar_4Glu_{12}/Orn_{12} micelles. After encapsulation of RNase followed by dialysis, we estimated the amount of RNase in the solution by Ag staining SDS-PAGE (Figure S8). The exact value cannot be calculated because it exceeds the detection limit, indicating a high amount of RNase remained in the solution. This result indicates that almost RNase was entrapped in the MAL-Sar_4Glu_{12}/Orn_{12} micelles.

Activity of RNase in the presence and absence of PICsome was measured by degradation of RNA (Figure 5 and Table S3).

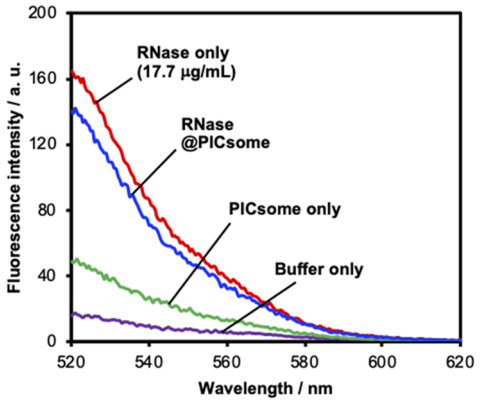

Figure 5. Fluorescent spectra for the substrate solution in the presence of RNase, RNase@PICsome, or PICsome after the enzyme activity assay.

RNA substrate was tagged with a fluorescent molecule on one end and a quencher on the other. The fluorescent molecule emits fluorescence at 520 nm by degradation of RNA mediated by RNase. DLS measurement revealed that the size of PICsome was maintained when the substrate RNA was added in the solution (Figure S9). This indicates that the substrate RNA did not disrupt the membrane of PICsome at this concentration. The fluorescence immediately increased within 5 min when the substrate was reacted with free RNase, showing the high activity of RNase. In the case of encapsulated RNase in PICsome, the fluorescence also increased after 5 min reaction, whereas only a slight increase was detected for PICsome without RNase (Figure 5). This result indicates that the encapsulated RNase kept the same level of enzymatic activity as the intact RNase. Since the membrane of PICsome is not cross-linked, oligoRNA can migrate into the membrane of PICsome in a dynamic equilibrium, and RNA in PICsome can attack the RNA. Therefore, we concluded that RNase was successfully encapsulated in the peptide-based PICsome without collapsing its protein structure responsible for its fluorescence property.

Finally, we investigated whether the peptide-based PICsome can deliver the encapsulated proteins into living plant cells. We previous reported that the delivery of PICsomes into plant cells requires modification of the PICsome with CPP.[11] The RNase-encapsulated PICsome (RNase@PICsome) was further modified with a CPP, KAibA (0.25 equiv to maleimide group, CKXAKXAKXA, X = Aib),[34] on the surface via a thiol-maleimide click reaction.[35] The artificial CPP KAibA was selected for the modification of PICsome due to the long-term cell-penetrating ability in both animal and plant cells as previously reported. Previously, we reported the postmodification of peptide/DNA complex micelles with CPP via maleimide-group-based click reaction. The postmodified micelle exhibited internalization efficiency in plant cells higher than that in the micelle modified with CPP prior to complexation.[35] The CPP modified to the peptide beforehand can cause undesired interactions, which results in collapse of micelles and vesicles. Thus, we modified PICsome with CPP after the preparation of PICsome. The modification efficiency of CPP at the maleimide groups on the surface of PICsome was estimated by HPLC without RNase (Figure S10). The chromatogram of Cys-KAibA and MAL-Sar_4-Glu_{12} showed a peak at 17 and 14.2 min, respectively. After the reaction, the chromatogram of the mixture of these peptides showed that a new peak appeared at 18.5 min, and the peak assigned to CPP completely disappeared. Thus, the reaction efficiency was determined to be 97.3% from the decrease in the peak area of KAibA peptide. In addition, MALDI-TOF-MS spectrum of the reaction mixture showed the exact mass corresponding to the product (Figure S11). The FE-SEM image of CPP-modified PICsome (CPP-PICsome) revealed that a spherical assembly was maintained after the modification with CPP (Figure S12). The CPP-modified PICsome containing RNase (RNase@CPP-PICsome) maintained the initial hydrodynamic diameter after the conjugation of CPP (Table 2 and Figure S13).

We infiltrated the solution of RNase@CPP-PICsome into 4-day-old seedlings of *Arabidopsis thaliana* by vacuum/compression method[36] and incubated the seedlings. Vacuum/compression method is useful to deliver various types of materials into a wide range of plants.[37] Using this method, micelles and vesicles can be sent to plants with high efficiency without damaging the plants. After incubation for 24 h, these

https://doi.org/10.1021/acspolymersau.1c00008
ACS Polym. Au 2021, 1, 30−38

Table 2. Z-Average Diameter of the CPP-PICsome, RNase@PICsome, and RNase@CPP-PICsome Obtained by DLS

	diameter[a] (nm)	PDI[b]
CPP-PICsome	171 ± 2	0.200
RNase@PICsome	208 ± 9	0.283
RNase@CPP-PICsome	220 ± 6	0.185

[a]Hydrodynamic diameter determined by DLS (n = 3). [b]Polydispersity index determined by DLS.

seedlings were observed by CLSM to confirm that RhB-RNase was internalized into the plant cells (Figure 6 and Figure S14).

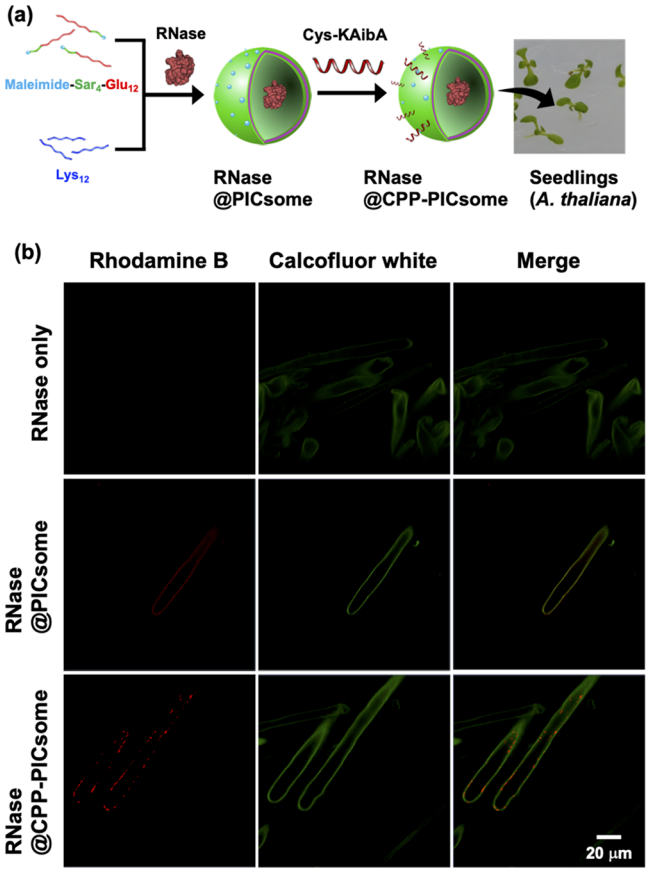

Figure 6. (a) Schematic illustration for encapsulation of a model protein, RNase, in PICsome followed by surface modification with cell penetrating peptide KAibA. The RNase-encapsulated PICsome (RNase@CPP-PICsome) was infiltrated into seedlings of *A. thaliana*. (b) Confocal microscopic images of *A. thaliana* root hair cells infiltrated with RNase only (20 μg mL^{-1}), RNase@PICsome, or RNase@CPP-PICsome. RhB labeled to RNase, red; calcofluor white, green.

The cell wall was stained with calcofluor white. When only RNase was infiltrated, no fluorescence was observed in the root hair cells. In the case of CPP-free RNase@PICsome, the red fluorescence from RhB was slightly observed and overlapped with the green signal of calcofluor white, indicating that PICsome was trapped on the cell walls without CPP modification. In contrast, strong dot-shaped fluorescence from RhB appeared inside the cell walls for the seedlings infiltrated with RNase@CPP-PICsome. We also introduced RNase@CPP-PICsome into YFP-expressing *A. thaliana* seedlings, in which YFP is expressed in the cytosol of plant cells. The fluorescence from RhB was overlapped with the fluorescence of YFP, indicating that RhB-modified RNase existed in the cytosol in plant cells (Figure S15). These results indicate that the PICsomes modified with KAibA at the surface can penetrate the cell wall and membrane and that RNase was then successfully internalized into the root cells. In addition, we evaluated native function of proteins encapsulated in PICsome inside of the plant cells. A yellow fluorescent protein (citrine) was encapsulated into PICsome in the same manner as RNase. The inclusion of citrine in PICsome was confirmed by FCS measurement, indicating that citrine kept its native fluorescing function inside PICsome (Figure S16). After modification with CPP to citrine@PICsome, the assembly was introduced to the *A. thaliana* seedlings. The CLSM observation of the seedlings revealed that the yellow fluorescence from citrine was confirmed inside plant cells (Figure S17). This result indicates that CPP-modified PICsome could transport proteins into plant cells and maintain their native functions.

We also evaluated cell viability of the seedlings infiltrated with CPP-PICsome by Evans blue assay. The amount of Evans blue adsorbed on the seedlings was determined by its absorbance after extraction. The cell viability was calculated by comparing the absorbance of Evans blue for the seedlings infiltered with water and each sample solution. The cell viability of seedlings infiltered with buffer only and CPP-PICsome solution was 99 and 90%, respectively (Figure 7).

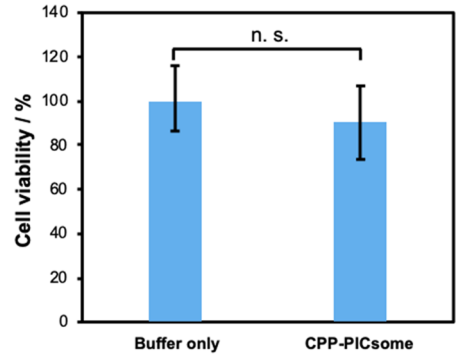

Figure 7. Evans blue assay of *A. thaliana* seedlings treated with Bis-Tris buffer or CPP-PICsome solution (100 μL). The cell viability of *A. thaliana* seedlings was obtained by standardizing the fluorescence of Evans blue extracted from the seedlings and averaging three replicates to determine the standard deviation. The P value was determined using the Mann−Whitney test, and a value of $P < 0.05$ was considered statistically significant: n.s.: not significant.

This revealed that the CPP-modified PICsome showed no significant toxicity to the *A. thaliana* seedlings. These results clearly show that PICsome modified with CPP can be safely applied as a protein delivery system to plant cells.

CONCLUSION

In conclusion, we developed novel PICsome from all-peptide-based components which are readily synthesized by solid-phase peptide synthesis. Combination of Lys and Glu dodecamers fused with the hydrophilic Sar tetramer enabled stable vesicle formation with a size of approximately 150 nm. The peptide-based PICsome was able to encapsulate RNase in its hollow structure with no influence on its enzyme activity, indicating

https://doi.org/10.1021/acspolymersau.1c00008
ACS Polym. Au 2021, 1, 30−38

that the peptide-based PICsome can be utilized for PEG-free platform for material delivery and/or nanoreactors in living systems. Modification at the maleimide groups displayed on the surface of PICsome is ongoing for further functionalization of PICsome.

■ ASSOCIATED CONTENT

Supporting Information

The Supporting Information is available free of charge at https://pubs.acs.org/doi/10.1021/acspolymersau.1c00008.

HPLC chromatograms for purified peptides and reaction mixture; MALDI-TOF-MS of purified peptides; *Z*-average diameter of the PICsome in the presence of NaCl or at various pH; size distribution of PICsome, CPP-PICsome, RNase@PICsome, and RNase@CPP-PICsome; size distribution of the mixture of PICsome and oligoRNA; MALDI-TOF-MS of the reaction mixture of PICsome and KAibA; normalized FCS curves for citrine in the absence (blue) and presence (red) of PICsome; CLSM images of seedlings (YFP over-expression *A. thaliana*) infiltrated with CPP-PICsome containing RhB-RNase; *Z*-stacked CLSM images of seedlings (*A. thaliana*) infiltrated with unmodified PICsome or CPP-PICsome containing RNase or citrine; quantification of RNase after dialysis by silver staining; FE-SEM image of the assembly formed from Arg_{12}/MAL-Sar_4Glu_{12} and CPP-modified PICsome; fluorescence intensity at 520 nm obtained from RNase activity assay (PDF)

■ AUTHOR INFORMATION

Corresponding Authors

Kousuke Tsuchiya − *Department of Material Chemistry, Graduate School of Engineering, Kyoto University, Kyoto 615-8510, Japan;* orcid.org/0000-0003-2364-8275; Email: tsuchiya.kosuke.3n@kyoto-u.ac.jp

Keiji Numata − *Department of Material Chemistry, Graduate School of Engineering, Kyoto University, Kyoto 615-8510, Japan; Biomacromolecules Research Team, RIKEN Center for Sustainable Resource Science, Saitama 351-0198, Japan;* orcid.org/0000-0003-2199-7420; Email: numata.keiji.3n@kyoto-u.ac.jp

Author

Seiya Fujita − *Department of Material Chemistry, Graduate School of Engineering, Kyoto University, Kyoto 615-8510, Japan*

Complete contact information is available at: https://pubs.acs.org/10.1021/acspolymersau.1c00008

Author Contributions

S.F. and K.T. are co-first authors. K.T. and K.N. conceived and designed the research. S.F. performed all the experiments and analyzed the data. All the authors wrote the manuscript.

Notes

The authors declare no competing financial interest.

■ ACKNOWLEDGMENTS

This work was supported by JST ERATO Grant No. JPMJER1602, Japan (K.N.) and JSPS KAKENHI Grant Nos. JP19K15643 (S.F.) and JP20K05636 (K.T.). We acknowledge the Support Unit for Bio-Material Analysis, RIKEN Center for Brain Science Research Resources Division, for performing the peptide syntheses.

■ REFERENCES

(1) Holowka, E. P.; Sun, V. Z.; Kamei, D. T.; Deming, T. J. Polyarginine Segments in Block Copolypeptides Drive Both Vesicular Assembly and Intracellular Delivery. *Nat. Mater.* **2007**, *6* (1), 52−57.

(2) Meng, F.; Zhong, Z.; Feijen, J. Stimuli-Responsive Polymersomes for Programmed Drug Delivery. *Biomacromolecules* **2009**, *10* (2), 197−209.

(3) Carlsen, A.; Lecommandoux, S. Self-Assembly of Polypeptide-Based Block Copolymer Amphiphiles. *Curr. Opin. Colloid Interface Sci.* **2009**, *14* (5), 329−339.

(4) Chen, H.; Xiao, L.; Anraku, Y.; Mi, P.; Liu, X.; Cabral, H.; Inoue, A.; Nomoto, T.; Kishimura, A.; Nishiyama, N.; Kataoka, K. Polyion Complex Vesicles for Photoinduced Intracellular Delivery of Amphiphilic Photosensitizer. *J. Am. Chem. Soc.* **2014**, *136* (1), 157−163.

(5) Rideau, E.; Dimova, R.; Schwille, P.; Wurm, F. R.; Landfester, K. Liposomes and polymersomes: a comparative review towards cell mimicking. *Chem. Soc. Rev.* **2018**, *47* (23), 8572−8610.

(6) Klermund, L.; Castiglione, K. Polymersomes as nanoreactors for preparative biocatalytic applications: current challenges and future perspectives. *Bioprocess Biosyst. Eng.* **2018**, *41* (9), 1233−1246.

(7) Anraku, Y.; Kishimura, A.; Oba, M.; Yamasaki, Y.; Kataoka, K. Spontaneous Formation of Nanosized Unilamellar Polyion Complex Vesicles with Tunable Size and Properties. *J. Am. Chem. Soc.* **2010**, *132* (5), 1631−1636.

(8) Koide, A.; Kishimura, A.; Osada, K.; Jang, W. D.; Yamasaki, Y.; Kataoka, K. Semipermeable polymer vesicle (PICsome) self-assembled in aqueous medium from a pair of oppositely charged block copolymers: Physiologically stable micro-/nanocontainers of water-soluble macromolecules. *J. Am. Chem. Soc.* **2006**, *128* (18), 5988−5989.

(9) Anraku, Y.; Kishimura, A.; Kamiya, M.; Tanaka, S.; Nomoto, T.; Toh, K.; Matsumoto, Y.; Fukushima, S.; Sueyoshi, D.; Kano, M. R.; Urano, Y.; Nishiyama, N.; Kataoka, K. Systemically Injectable Enzyme-Loaded Polyion Complex Vesicles as In Vivo Nanoreactors Functioning in Tumors. *Angew. Chem., Int. Ed.* **2016**, *55* (2), 560−565.

(10) Kishimura, A.; Koide, A.; Osada, K.; Yamasaki, Y.; Kataoka, K. Encapsulation of myoglobin in PEGylated polyion complex vesicles made from a pair of oppositely charged block lonomers: A physiologically available oxygen carrier. *Angew. Chem., Int. Ed.* **2007**, *46* (32), 6085−6088.

(11) Fujita, S.; Motoda, Y.; Kigawa, T.; Tsuchiya, K.; Numata, K. Peptide-based polyion complex vesicles that deliver enzymes into intact plants to provide antibiotic resistance without genetic modifications. *Biomacromolecules* **2021**, *22* (3), 1080−1090.

(12) Wang, J. Z.; You, M. L.; Ding, Z. Q.; Ye, W. B. A review of emerging bone tissue engineering via PEG conjugated biodegradable amphiphilic copolymers. *Mater. Sci. Eng., C* **2019**, *97*, 1021−1035.

(13) Rahme, K.; Dagher, N. Chemistry Routes for Copolymer Synthesis Containing PEG for Targeting, Imaging, and Drug Delivery Purposes. *Pharmaceutics* **2019**, *11* (7), 327.

(14) Hu, Y. L.; Hou, Y. Q.; Wang, H.; Lu, H. Polysarcosine as an Alternative to PEG for Therapeutic Protein Conjugation. *Bioconjugate Chem.* **2018**, *29* (7), 2232−2238.

(15) Pelegri-O'Day, E. M.; Lin, E.-W.; Maynard, H. D. Therapeutic Protein-Polymer Conjugates: Advancing Beyond PEGylation. *J. Am. Chem. Soc.* **2014**, *136* (41), 14323−14332.

(16) Khutoryanskiy, V. V. Beyond PEGylation: Alternative surface-modification of nanoparticles with mucus-inert biomaterials. *Adv. Drug Delivery Rev.* **2018**, *124*, 140−149.

(17) Heller, P.; Mohr, N.; Birke, A.; Weber, B.; Reske-Kunz, A.; Bros, M.; Barz, M. Directed Interactions of Block Copolypept(o) ides

with Mannose-Binding Receptors: PeptoMicelles Targeted to Cells of the Innate Immune System. *Macromol. Biosci.* **2015**, *15* (1), 63−73.
(18) Birke, A.; Huesmann, D.; Kelsch, A.; Weilbacher, M.; Xie, J.; Bros, M.; Bopp, T.; Becker, C.; Landfester, K.; Barz, M. Polypeptoid-block-polypeptide Copolymers: Synthesis, Characterization, and Application of Amphiphilic Block Copolypept(o)ides in Drug Formulations and Miniemulsion Techniques. *Biomacromolecules* **2014**, *15* (2), 548−557.
(19) Yamamoto, F.; Yamahara, R.; Makino, A.; Kurihara, K.; Tsukada, H.; Hara, E.; Hara, I.; Kizaka-Kondoh, S.; Ohkubo, Y.; Ozeki, E.; Kimura, S. Radiosynthesis and initial evaluation of F-18 labeled nanocarrier composed of poly(L-lactic acid)-*block*-poly-(sarcosine) amphiphilic polydepsipeptide. *Nucl. Med. Biol.* **2013**, *40* (3), 387−394.
(20) Kidchob, T.; Kimura, S.; Imanishi, Y. Amphiphilic poly(Ala)-*b*-poly(Sar) microspheres loaded with hydrophobic drug. *J. Controlled Release* **1998**, *51* (2−3), 241−248.
(21) Matsui, H.; Ueda, M.; Makino, A.; Kimura, S. Molecular assembly composed of a dendrimer template and block polypeptides through stereocomplex formation. *Chem. Commun.* **2012**, *48* (49), 6181−6183.
(22) Aoi, K.; Hatanaka, T.; Tsutsumiuchi, K.; Okada, M.; Imae, T. Synthesis of a novel star-shaped dendrimer by radial-growth polymerization of sarcosine *N*-carboxyanhydride initiated with poly(trimethyleneimine) dendrimer. *Macromol. Rapid Commun.* **1999**, *20* (7), 378−382.
(23) Tao, X. F.; Chen, H.; Trepout, S.; Cen, J. Y.; Ling, J.; Li, M. H. Polymersomes with aggregation-induced emission based on amphiphilic block copolypeptoids. *Chem. Commun.* **2019**, *55* (90), 13530−13533.
(24) Deng, Y. W.; Chen, H.; Tao, X. F.; Cao, F. Y.; Trepout, S.; Ling, J.; Li, M. H. Oxidation-Sensitive Polymersomes Based on Amphiphilic Diblock Copolypeptoids. *Biomacromolecules* **2019**, *20* (9), 3435−3444.
(25) Bleher, S.; Buck, J.; Muhl, C.; Sieber, S.; Barnert, S.; Witzigmann, D.; Huwyler, J.; Barz, M.; Suss, R. Poly(Sarcosine) Surface Modification Imparts Stealth-Like Properties to Liposomes. *Small* **2019**, *15* (50), 1904716.
(26) Ueda, M.; Makino, A.; Imai, T.; Sugiyama, J.; Kimura, S. Temperature-Triggered Fusion of Vesicles Composed of Right-Handed and Left-Handed Amphiphilic Helical Peptides. *Langmuir* **2011**, *27* (8), 4300−4304.
(27) Makino, A.; Yamahara, R.; Ozeki, E.; Kimura, S. Preparation of novel polymer assemblies, "lactosome", composed of Poly(L-lactic acid) and poly(sarcosine). *Chem. Lett.* **2007**, *36* (10), 1220−1221.
(28) Chan, B. A.; Xuan, S. T.; Li, A.; Simpson, J. M.; Sternhagen, G. L.; Yu, T. Y.; Darvish, O. A.; Jiang, N. S.; Zhang, D. H. Polypeptoid polymers: Synthesis, characterization, and properties. *Biopolymers* **2018**, *109* (1), No. e23070.
(29) Birke, A.; Ling, J.; Barz, M. Polysarcosine-containing copolymers: Synthesis, characterization, self-assembly, and applications. *Prog. Polym. Sci.* **2018**, *81*, 163−208.
(30) Khuphe, M.; Mahon, C. S.; Thornton, P. D. Glucose-Bearing Biodegradable Poly(Amino Acid) and Poly(Amino Acid)-Poly(Ester) Conjugates for Controlled Payload Release. *Biomater. Sci.* **2016**, *4* (12), 1792−1801.
(31) Ulbricht, J.; Jordan, R.; Luxenhofer, R. On the Biodegradability of Polyethylene Glycol, Polypeptoids and Poly(2-Oxazoline)S. *Biomaterials* **2014**, *35* (17), 4848−4861.
(32) Chuanoi, S.; Kishimura, A.; Dong, W. F.; Anraku, Y.; Yamasaki, Y.; Kataoka, K. Structural factors directing nanosized polyion complex vesicles (Nano-PICsomes) to form a pair of block aniomer/homo catiomers: studies on the aniomer segment length and the catiomer side-chain structure. *Polym. J.* **2014**, *46* (2), 130−135.
(33) Rao, M. V. R.; Atreyi, M.; Rajeswari, M. R. Specific interactions between amino acid side chains - A partial molar volume study. *Can. J. Chem.* **1988**, *66* (3), 487−490.
(34) Terada, K.; Gimenez-Dejoz, J.; Miyagi, Y.; Oikawa, K.; Tsuchiya, K.; Numata, K. Artificial Cell-Penetrating Peptide Containing Periodic α-Aminoisobutyric Acid with Long-Term Internalization Efficiency in Human and Plant Cells. *ACS Biomater. Sci. Eng.* **2020**, *6* (6), 3287−3298.
(35) Miyamoto, T.; Tsuchiya, K.; Numata, K. Block Copolymer/Plasmid DNA Micelles Postmodified with Functional Peptides via Thiol-Maleimide Conjugation for Efficient Gene Delivery into Plants. *Biomacromolecules* **2019**, *20* (2), 653−661.
(36) Midorikawa, K.; Kodama, Y.; Numata, K. Vacuum/Compression Infiltration-mediated Permeation Pathway of a Peptide-pDNA Complex as a Non-Viral Carrier for Gene Delivery in Planta. *Sci. Rep.* **2019**, *9* (1), 271.
(37) Watanabe, K.; Odahara, M.; Miyamoto, T.; Numata, K. Fusion Peptide-Based Biomacromolecule Delivery System for Plant Cells. *ACS Biomater. Sci. Eng.* **2021**, DOI: 10.1021/acsbiomaterials.1c00227.